Table 2.3.5.1. *Possible types of vector searches*

Self-vectors	Cross-vectors	Dimension of search, n
(1) Locate single site relative to particle centre		$n = 3$
(2)	Use information from (1) to locate particle centre	$n \leq 3$
(3) Simultaneous search for both (1) and (2). In general this is a six-dimensional search but may be simplified when particle is on a crystallographic symmetry axis		$3 \leq n \leq 6$
(4) Given (1) for more than one site, find all vectors within particle		$n = 3$
(5) Given information from (3), locate additional site using complete vector set		$n = 3$

heavy-atom position was assigned (atom A_2 at x, y, z). At this juncture, the known noncrystallographic symmetry was used to obtain a full interpretation. From Table 2.3.5.2 we see that molecular axis 2 will generate a second heavy atom with coordinates roughly $\frac{1}{4}+y, -\frac{1}{4}+x, 2Z-z$ (if the molecular centre was assumed to be at $\frac{1}{2}, \frac{1}{4}, Z$). Starting from the tentative coordinates of site A_2, the site A_1 related by molecular axis 1 was detected at about the predicted position and the second site A_1 generated acceptable cross-vectors with the earlier determined site A_2. Further examination enabled the completion of the set of four noncrystallographically related heavy-atom sites, such that all predicted Patterson vectors were acceptable and all four sites placed the molecular centre in the same position. Following refinement of these four sites, the corresponding SIR phases were used to find an additional set of four sites in this compound as well as in a number of other derivatives. The multiple isomorphous replacement phases, in conjunction with real-space electron-density averaging of the noncrystallographically related units, were then sufficient to solve the GAPDH structure.

When investigators studied larger macromolecular aggregates such as the icosahedral viruses, which have 532 point symmetry, systematic methods were developed for utilizing the noncrystallographic symmetry to aid in locating heavy-atom sites in isomorphous heavy-atom derivatives. Argos & Rossmann (1974, 1976) introduced an exhaustive Patterson search procedure for a single heavy-atom site within the noncrystallographic asymmetric unit which has been successfully applied to the interpretation of both virus [satellite tobacco necrosis virus (STNV) (Lentz *et al.*, 1976), southern bean mosaic virus (Rayment *et al.*, 1978), alfalfa mosaic virus (Fukuyama *et al.*, 1983), cowpea mosaic virus (Stauffacher *et al.*, 1987)] and enzyme [catalase (Murthy *et al.*, 1981)] heavy-atom difference Pattersons. A heavy atom is placed in turn at all plausible positions within the volume of the noncrystallographic asymmetric unit and the corresponding vector set is constructed from the resulting constellation of heavy atoms. Argos & Rossmann (1976) found a spherical polar coordinate search grid to be convenient for spherical viruses. After all vectors for the current search position are predicted, the vectors are allocated to the nearest grid point and the list is sorted to eliminate recurring ones. The criterion used by Argos & Rossmann for selecting a solution is that the sum

$$S = \sum_{i=1}^{N} P_i - NP_{\rm av}$$

of the lookup Patterson density values P_i achieves a high value for a correct heavy-atom position. The sum is corrected for the carpet of cross-vectors by the second term in the sum.

An additional criterion, which has been found useful for discriminating correct solutions, is a unit vector density criterion

$$U = \sum_{i=1}^{N} (P_i/n_i) \Big/ N,$$

where n_i is the number of vectors expected to contribute to the Patterson density value P_i (Arnold *et al.*, 1987). This criterion can be especially valuable for detecting correct solutions at special search positions, such as an icosahedral fivefold axis, where the number of vector lookup positions may be drastically reduced owing to the higher symmetry. An alternative, but equivalent, method for locating heavy-atom positions from isomorphous difference data is discussed in Section 2.3.3.5.

Even for a single heavy-atom site at a general position in the simplest icosahedral or $(T = 1)$ virus, there are 60 equivalent heavy atoms in one virus particle. The number of unique vectors corresponding to this self-particle vector set will depend on the crystal symmetry but may be as many as $(60)(59)/2 = 1770$ for a virus particle at a general crystallographic position. Such was the case for the STNV crystals which were in space group $C2$ containing four virus particles at general positions. The method of Argos & Rossmann was applied successfully to a solution of the K_2HgI_4 derivative of STNV using a 10 Å resolution difference Patterson. Application of the noncrystallographic symmetry vector search procedure to a $K_2Au(CN)_2$ derivative of human rhinovirus 14 (HRV14) crystals (space group $P2_13, Z = 4$) has succeeded in establishing both the relative positions of heavy atoms within one particle and the positions of the virus particles relative to the crystal symmetry elements (Arnold *et al.*, 1987). The particle position was established by incorporating interparticle vectors in the search and varying the particle position along the crystallographic threefold axis until the best fit for the predicted vector set was achieved.

Table 2.3.5.2. *Orientation of the glyceraldehyde-3-phosphate dehydrogenase molecular twofold axis in the orthorhombic cell*

Rotation axes	Polar coordinates (°)		Cartesian coordinates (direction cosines)		
	ψ	φ	u	v	w
1	45.0	−7.0	0.7018	0.7071	−0.0862
2	180.0–55.0	38.6	0.6402	−0.5736	0.5111
3	180.0–66.0	−70.6	0.3035	−0.4067	−0.8616

2.3.6. Rotation functions

2.3.6.1. *Introduction*

The rotation function is designed to detect noncrystallographic rotational symmetry (see Table 2.3.6.1). The normal rotation function definition is given as (Rossmann & Blow, 1962)

$$R = \int_U P_1(\mathbf{u}) \cdot P_2(\mathbf{u}')\, {\rm d}\mathbf{u}, \qquad (2.3.6.1)$$

where P_1 and P_2 are two Pattersons and U is an envelope centred at the superimposed origins. This convolution therefore measures the degree of similarity, or 'overlap', between the two Pattersons when P_2 has been rotated relative to P_1 by an amount defined by

Copyright © 2006 International Union of Crystallography

Table 2.3.6.1. *Different types of uses for the rotation function*

Type of rotation function	Pattersons to be compared		Purpose
	P_1	P_2	
Self	Unknown structure	Unknown structure, same cell	Finds orientation of noncrystallographic axes
Cross	Unknown structure	Unknown structure in different cell	Finds relative orientation of unknown molecules
Cross	Unknown structure	Known structure in large cell to avoid overlap of self-Patterson vectors	Determines orientation of unknown structure as preliminary to positioning and subsequent phasing with known molecule

$$\mathbf{u}' = [\boldsymbol{C}]\mathbf{u}. \tag{2.3.6.2}$$

The elements of $[\boldsymbol{C}]$ will depend on three rotation angles $(\theta_1, \theta_2, \theta_3)$. Thus, R is a function of these three angles. Alternatively, the matrix $[\boldsymbol{C}]$ could be used to express mirror symmetry, permitting searches for noncrystallographic mirror or glide planes.

The basic concepts were first clearly stated by Rossmann & Blow (1962), although intuitive uses of the rotation function had been considered earlier. Hoppe (1957*b*) had also hinted at a convolution of the type given by (2.3.6.1) to find the orientation of known molecular fragments and these ideas were implemented by Huber (1965).

Consider a structure of two identical units which are in different orientations. The Patterson function of such a structure consists of three parts. There will be the self-Patterson vectors of one unit, being the set of interatomic vectors which can be formed within that unit, with appropriate weights. The set of self-Patterson vectors of the other unit will be identical, but they will be rotated away from the first due to the different orientation. Finally, there will be the cross-Patterson vectors, or set of interatomic vectors which can be formed from one unit to another. The self-Patterson vectors of the two units will all lie in a volume centred at the origin and limited by the overall dimensions of the units. Some or all of the cross-Patterson vectors will lie outside this volume. Suppose the Patterson function is now superposed on a rotated version of itself. There will be no particular agreement except when one set of self-Patterson vectors of one unit has the same orientation as the self-Patterson vectors from the other unit. In this position, we would expect a maximum of agreement or 'overlap' between the two. Similarly, the superposition of the molecular self-Patterson derived from different crystal forms can provide the relative orientation of the two crystals when the molecules are aligned.

While it would be possible to evaluate R by interpolating in P_2 and forming the point-by-point product with P_1 within the volume U for every combination of θ_1, θ_2 and θ_3, such a process is tedious and requires large computer storage for the Pattersons. Instead, the process is usually performed in reciprocal space where the number of independent structure amplitudes which form the Pattersons is about one-thirtieth of the number of Patterson grid points. Thus, the computation of a rotation function is carried out directly on the structure amplitudes, while the overlap definition (2.3.6.1) simply serves as a physical basis for the technique.

The derivation of the reciprocal-space expression depends on the expansion of each Patterson either as a Fourier summation, the conventional approach of Rossmann & Blow (1962), or as a sum of spherical harmonics in Crowther's (1972) analysis. The conventional and mathematically easier treatment is discussed presently, but the reader is referred also to Section 2.3.6.5 for Crowther's elegant approach. The latter leads to a rapid technique for performing the computations, about one hundred times faster than conventional methods.

Let, omitting constant coefficients,

$$P_1(\mathbf{u}) = \sum_{\mathbf{h}} |\mathbf{F}_\mathbf{h}|^2 \ \exp\ (2\pi i \mathbf{h}\cdot\mathbf{u})$$

and

$$P_2(\mathbf{u}') = \sum_{\mathbf{p}} |\mathbf{F}_\mathbf{p}|^2 \ \exp\ (2\pi i \mathbf{p}\cdot\mathbf{u}').$$

From (2.3.6.2) it follows that

$$P_2(\mathbf{u}') = \sum_{\mathbf{p}} |\mathbf{F}_\mathbf{p}|^2 \ \exp\ (2\pi i \mathbf{p}[\boldsymbol{C}]\cdot\mathbf{u}),$$

and, hence, by substitution in (2.3.6.1)

$$\begin{aligned} R(\theta_1,\theta_2,\theta_3) &= \int_U \left[\sum_{\mathbf{h}} |\mathbf{F}_\mathbf{h}|^2 \ \exp\ (2\pi i \mathbf{h}\cdot\mathbf{u})\right] \\ &\quad \times \left[\sum_{\mathbf{p}} |\mathbf{F}_\mathbf{p}|^2 \ \exp\ (2\pi i \mathbf{p}[\boldsymbol{C}]\cdot\mathbf{u})\right] \mathrm{d}\mathbf{u} \\ &= U\sum_{\mathbf{h}} |\mathbf{F}_\mathbf{h}|^2 \left(\sum_{\mathbf{p}} |\mathbf{F}_\mathbf{p}|^2 G_{\mathbf{hp}}\right), \end{aligned} \tag{2.3.6.3}$$

where

$$UG_{\mathbf{hp}} = \int_U \exp\ \{2\pi i(\mathbf{h} + \mathbf{p}[\boldsymbol{C}])\cdot\mathbf{u}\}\ \mathrm{d}\mathbf{u}.$$

When the volume U is a sphere, $G_{\mathbf{hp}}$ has the analytical form

$$G_{\mathbf{hp}} = \frac{3(\sin\theta - \theta\ \cos\ \theta)}{\theta^3}, \tag{2.3.6.4}$$

where $\theta = 2\pi HR$ and $H = \mathbf{h} + \mathbf{p}[\boldsymbol{C}]$. G is a spherical interference function whose form is shown in Fig. 2.3.6.1

The expression (2.3.6.3) represents the rotation function in reciprocal space. If $\mathbf{h}' = [\boldsymbol{C}^T]\mathbf{p}$ in the argument of $G_{\mathbf{hp}}$, then $\mathbf{h}'$ can be seen as the point in reciprocal space to which $\mathbf{p}$ is rotated by $[\boldsymbol{C}]$. Only for those integral reciprocal-lattice points which are close to $\mathbf{h}'$ will $G_{\mathbf{hp}}$ be of an appreciable size (Fig. 2.3.6.1). Thus, the number of significant terms is greatly reduced in the summation over $\mathbf{p}$ for every value of $\mathbf{h}$, making the computation of the rotation function manageable.

The radius of integration R should be approximately equal to or a little smaller than the molecular diameter. If R were roughly equal to the length of a lattice translation, then the separation of reciprocal-lattice points would be about $1/R$. Hence, when H is equal to one reciprocal-lattice separation, $HR \simeq 1$, and G is thus

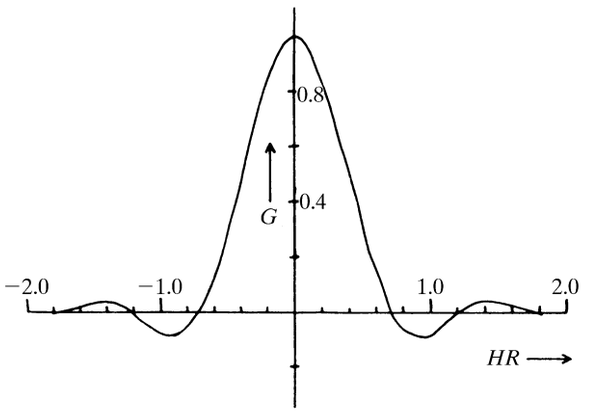

Fig. 2.3.6.1. Shape of the interference function G for a spherical envelope of radius R at a distance H from the reciprocal-space origin. [Reprinted from Rossmann & Blow (1962).]

quite small. Indeed, all terms with $HR > 1$ might well be neglected. Thus, in general, the only terms that need be considered are those where $-\mathbf{h}'$ is within one lattice point of $\mathbf{h}$. However, in dealing with a small molecular fragment for which R is small compared to the unit-cell dimensions, more reciprocal-lattice points must be included for the summation over $\mathbf{p}$ in the rotation-function expression (2.3.6.3).

In practice, the equation

$$\mathbf{h} + \mathbf{h}' = 0,$$

that is

$$[\boldsymbol{C}^T]\mathbf{p} = -\mathbf{h}$$

or

$$\mathbf{p} = [\boldsymbol{C}^T]^{-1}(-\mathbf{h}), \tag{2.3.6.5}$$

determines $\mathbf{p}$, given a set of Miller indices $\mathbf{h}$. This will give a non-integral set of Miller indices. The terms included in the inner summation of (2.3.6.3) will be integral values of $\mathbf{p}$ around the non-integral lattice point found by solving (2.3.6.5).

Details of the conventional program were given by Tollin & Rossmann (1966) and follow the principles outlined above. They discussed various strategies as to which crystal should be used to calculate the first ($\mathbf{h}$) and second ($\mathbf{p}$) Patterson. Rossmann & Blow (1962) noted that the factor $\sum_{\mathbf{p}}|\mathbf{F}_{\mathbf{p}}|^2 G_{\mathbf{hp}}$ in expression (2.3.6.3) represents an interpolation of the squared transform of the self-Patterson of the second ($\mathbf{p}$) crystal. Thus, the rotation function is a sum of the products of the two molecular transforms taken over all the $\mathbf{h}$ reciprocal-lattice points. Lattman & Love (1970) therefore computed the molecular transform explicitly and stored it in the computer, sampling it as required by the rotation operation. A discussion on the suitable choice of variables in the computation of rotation functions has been given by Lifchitz (1983).

2.3.6.2. *Matrix algebra*

The initial step in the rotation-function procedure involves the orthogonalization of both crystal systems. Thus, if fractional coordinates in the first crystal system are represented by $\mathbf{x}$, these can be orthogonalized by a matrix $[\beta]$ to give the coordinates $\mathbf{X}$ in units of length (Fig. 2.3.6.2); that is,

$$\mathbf{X} = [\boldsymbol{\beta}]\mathbf{x}.$$

If the point $\mathbf{X}$ is rotated to the point $\mathbf{X}'$, then

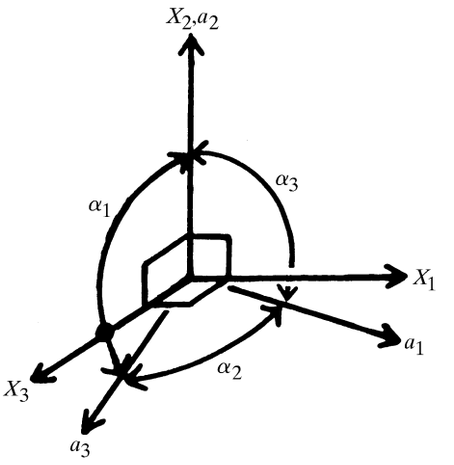

Fig. 2.3.6.2. Relationships of the orthogonal axes X_1, X_2, X_3 to the crystallographic axes a_1, a_2, a_3. [Reprinted from Rossmann & Blow (1962).]

$$\mathbf{X}' = [\boldsymbol{\rho}]\mathbf{X}, \tag{2.3.6.6}$$

where $\boldsymbol{\rho}$ represents the rotation matrix relating the two vectors in the orthogonal system. Finally, $\mathbf{X}'$ is converted back to fractional coordinates measured along the oblique cell dimension in the second crystal by

$$\mathbf{x}' = [\boldsymbol{\alpha}]\mathbf{X}'.$$

Thus, by substitution,

$$\mathbf{x}' = [\boldsymbol{\alpha}][\boldsymbol{\rho}]\mathbf{X} = [\boldsymbol{\alpha}][\boldsymbol{\rho}][\boldsymbol{\beta}]\mathbf{x}, \tag{2.3.6.7}$$

and by comparison with (2.3.6.2) it follows that

$$[\boldsymbol{C}] = [\boldsymbol{\alpha}][\boldsymbol{\rho}][\boldsymbol{\beta}].$$

Fig. 2.3.6.2 shows the mode of orthogonalization used by Rossmann & Blow (1962). With their definition it can be shown that

$$[\boldsymbol{\alpha}] = \begin{pmatrix} 1/(a_1 \sin\alpha_3 \sin\omega) & 0 & 0 \\ 1/(a_2 \tan\alpha_1 \tan\omega) & 1/a_2 & -1/(a_2 \tan\alpha_1) \\ -1/(a_2 \tan\alpha_3 \sin\omega) & & \\ -1/(a_3 \sin\alpha_1 \tan\omega) & 0 & 1/(a_3 \sin\alpha_1) \end{pmatrix}$$

and

$$[\boldsymbol{\beta}] = \begin{pmatrix} a_1 \sin\alpha_3 \sin\omega & 0 & 0 \\ a_1 \cos\alpha_3 & a_2 & a_3 \cos\alpha_1 \\ a_1 \sin\alpha_3 \cos\omega & 0 & a_3 \sin\alpha_1 \end{pmatrix},$$

where $\cos\omega = (\cos\alpha_2 - \cos\alpha_1 \cos\alpha_3)/(\sin\alpha_1 \sin\alpha_3)$ with $0 \le \omega < \pi$. For a Patterson compared with itself, $[\boldsymbol{\alpha}] = [\boldsymbol{\beta}]^{-1}$.

Both spherical (κ, ψ, φ) and Eulerian $(\theta_1, \theta_2, \theta_3)$ angles are used in evaluating the rotation function. The usual definitions employed are given diagrammatically in Figs. 2.3.6.3 and 2.3.6.4. They give rise to the following rotation matrices.

(*a*) Matrix $[\boldsymbol{\rho}]$ in terms of Eulerian angles $\theta_1, \theta_2, \theta_3$:

$$\begin{pmatrix} -\sin\theta_1 \cos\theta_2 \sin\theta_3 + \cos\theta_1 \cos\theta_3 & \cos\theta_1 \cos\theta_2 \sin\theta_3 + \sin\theta_1 \cos\theta_3 & \sin\theta_2 \sin\theta_3 \\ -\sin\theta_1 \cos\theta_2 \cos\theta_3 - \cos\theta_1 \sin\theta_3 & \cos\theta_1 \cos\theta_2 \cos\theta_3 - \sin\theta_1 \sin\theta_3 & \sin\theta_2 \cos\theta_3 \\ \sin\theta_1 \sin\theta_2 & -\cos\theta_1 \sin\theta_2 & \cos\theta_2 \end{pmatrix}$$

and (*b*) matrix $[\boldsymbol{\rho}]$ in terms of rotation angle κ and the spherical polar coordinates ψ, φ:

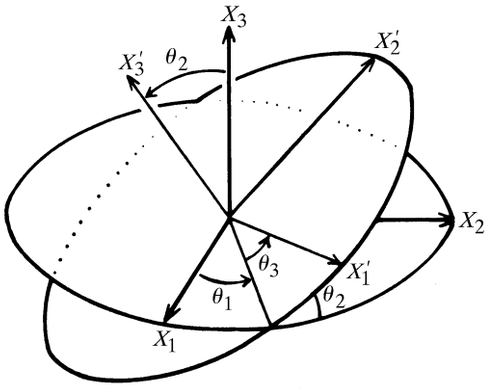

Fig. 2.3.6.3. Eulerian angles $\theta_1, \theta_2, \theta_3$ relating the rotated axes X_1', X_2', X_3' to the original unrotated orthogonal axes X_1, X_2, X_3. [Reprinted from Rossmann & Blow (1962).]

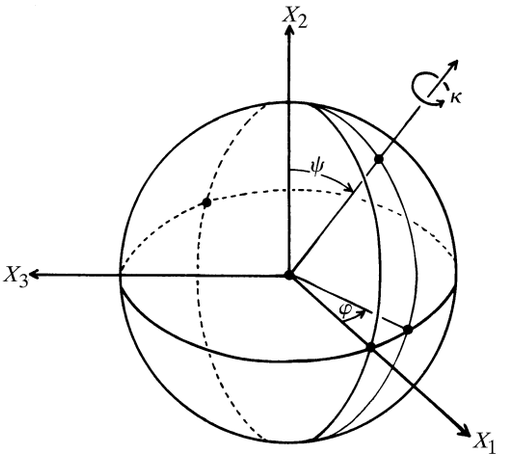

Fig. 2.3.6.4. Variables ψ and φ are polar coordinates which specify a direction about which the axes may be rotated through an angle κ. [Reprinted from Rossmann & Blow (1962).]

$$\begin{pmatrix} \cos\kappa + \sin^2\psi\cos^2\varphi(1-\cos\kappa) & \sin\psi\cos\psi\cos\varphi(1-\cos\kappa) + \sin\psi\sin\varphi\sin\kappa & \\ \sin\psi\cos\psi\cos\varphi(1-\cos\kappa) - \sin\psi\sin\varphi\sin\kappa & \cos\kappa + \cos^2\psi(1-\cos\kappa) & \\ -\sin^2\psi\sin\varphi\cos\varphi(1-\cos\kappa) - \cos\psi\sin\kappa & -\sin\psi\cos\psi\sin\varphi(1-\cos\kappa) + \sin\psi\cos\varphi\sin\kappa & \end{pmatrix}$$
$$\begin{pmatrix} -\sin^2\psi\cos\varphi\sin\varphi(1-\cos\kappa) + \cos\psi\sin\kappa \\ -\sin\psi\cos\psi\sin\varphi(1-\cos\kappa) - \sin\psi\cos\varphi\sin\kappa \\ \cos\kappa + \sin^2\psi\sin^2\varphi(1-\cos\kappa) \end{pmatrix}$$

Alternatively, (b) can be expressed as

$$\begin{pmatrix} \cos\kappa + u^2(1-\cos\kappa) & uv(1-\cos\kappa) - w\sin\kappa & \\ vu(1-\cos\kappa) + w\sin\kappa & \cos\kappa + v^2(1-\cos\kappa) & \\ wu(1-\cos\kappa) - v\sin\kappa & wv(1-\cos\kappa) + u\sin\kappa & \end{pmatrix}$$
$$\begin{pmatrix} uw(1-\cos\kappa) + v\sin\kappa \\ uw(1-\cos\kappa) - u\sin\kappa \\ \cos\kappa + w^2(1-\cos\kappa) \end{pmatrix},$$

where u, v and w are the direction cosines of the rotation axis given by

$$u = \sin\psi\cos\varphi,$$
$$v = \cos\psi,$$
$$w = -\sin\psi\sin\varphi.$$

This latter form also demonstrates that the trace of a rotation matrix is $2\cos\kappa + 1$.

The relationship between the two sets of variables established by comparison of the elements of the two matrices yields

$$\cos(\kappa/2) = \cos(\theta_2/2)\cos\left(\frac{\theta_1+\theta_3}{2}\right),$$
$$\tan\varphi = -\cot(\theta_2/2)\sin\left(\frac{\theta_1+\theta_3}{2}\right)\sec\left(\frac{\theta_1-\theta_3}{2}\right),$$
$$\cos\varphi\tan\psi = \cot\left(\frac{\theta_1-\theta_3}{2}\right).$$

Since φ and ψ can always be chosen in the range 0 to π, these equations suffice to find (κ, ψ, φ) from any set $(\theta_1, \theta_2, \theta_3)$.

2.3.6.3. *Symmetry*

In analogy with crystal lattices, the rotation function is periodic and contains symmetry. The rotation function has a cell whose periodicity is 2π in each of its three angles. This may be written as

$$R(\theta_1, \theta_2, \theta_3) \equiv R(\theta_1 + 2\pi n_1, \theta_2 + 2\pi n_2, \theta_3 + 2\pi n_3)$$

or

$$R(\kappa, \psi, \varphi) \equiv R(\kappa + 2\pi n_1, \psi + 2\pi n_2, \varphi + 2\pi n_3),$$

where n_1, n_2 and n_3 are integers. A redundancy in the definition of either set of angles leads to the equivalence of the following points:

$$R(\theta_1, \theta_2, \theta_3) \equiv R(\theta_1 + \pi, -\theta_2, \theta_3 + \pi) \quad \text{in Eulerian space}$$

or

$$R(\kappa, \psi, \varphi) \equiv R(\kappa, 2\pi - \psi, \varphi + \pi) \quad \text{in polar space.}$$

These relationships imply an n glide plane perpendicular to θ_2 for Eulerian space or a φ glide plane perpendicular to ψ in polar space.

In addition, the Laue symmetry of the two Pattersons themselves must be considered. This problem was first discussed by Rossmann & Blow (1962) and later systematized by Tollin *et al.* (1966), Burdina (1970, 1971, 1973) and Rao *et al.* (1980). A closely related problem was considered by Hirshfeld (1968). The rotation function will have the same value whether the Patterson density at $\mathbf{X}$ or $[\boldsymbol{T}_i]\mathbf{X}$ in the first crystal is multiplied by the Patterson density at $\mathbf{X}'$ or $[\boldsymbol{T}_j]\mathbf{X}'$ in the second crystal. $[\boldsymbol{T}_i]$ and $[\boldsymbol{T}_j]$ refer to the ith and jth crystallographic rotations in the orthogonalized coordinate systems of the first and second crystal, respectively. Hence, from (2.3.6.6)

$$([\boldsymbol{T}_j]\mathbf{X}') = [\boldsymbol{\rho}]([\boldsymbol{T}_i]\mathbf{X})$$

or

Table 2.3.6.2. *Eulerian symmetry elements for all possible types of space-group rotations*

Axis	Direction	First crystal	Second crystal
1		$(\pi+\theta_1, -\theta_2, \pi+\theta_3)$	$(\pi+\theta_1, -\theta_2, \pi+\theta_3)$
2	[010]	$(\pi-\theta_1, \pi+\theta_2, \theta_3)$	$(\theta_1, \pi+\theta_2, \pi-\theta_3)$
2	[001]	$(\pi+\theta_1, \theta_2, \theta_3)$	$(\theta_1, \theta_2, \pi+\theta_3)$
4	[001]	$(-\pi/2+\theta_1, \theta_2, \theta_3)$	$(\theta_1, \theta_2, \pi/2+\theta_3)$
3	[001]	$(-2\pi/3+\theta_1, \theta_2, \theta_3)$	$(\theta_1, \theta_2, 2\pi/3+\theta_3)$
6	[001]	$(-\pi/3+\theta_1, \theta_2, \theta_3)$	$(\theta_1, \theta_2, \pi/3+\theta_3)$
2*	[110]	$(3\pi/2-\theta_1, \pi-\theta_2, \pi+\theta_3)$	$(\pi+\theta_1, \pi-\theta_2, -3\pi/2-\theta_3)$

* This axis is not unique (that is, it can always be generated by two other unique axes), but is included for completeness.

$$\mathbf{X}' = [\boldsymbol{T}_j^T][\boldsymbol{\rho}][\boldsymbol{T}_i]\mathbf{X}.$$

Thus, it is necessary to find angular relationships which satisfy the relation

$$[\boldsymbol{\rho}] = [\boldsymbol{T}_j^T][\boldsymbol{\rho}][\boldsymbol{T}_i]$$

for given Patterson symmetries. Tollin *et al*. (1966) show that the Eulerian angular equivalences can be expressed in terms of the Laue symmetries of each Patterson (Table 2.3.6.2).

The example given by Tollin *et al*. (1966) is instructive in the use of Table 2.3.6.2. They consider the determination of the Eulerian space group when P_1 has symmetry *Pmmm* and P_2 has symmetry $P2/m$. These Pattersons contain the proper rotation groups 222 and 2 (parallel to **b**), respectively. Inspection of Table 2.3.6.2 shows that these symmetries produce the following Eulerian relationships:

(*a*) In the first crystal (*Pmmm*):

$\theta_1\theta_2\theta_3 \rightarrow \pi+\theta_1, -\theta_2, \pi+\theta_3$ (onefold axis)

$\theta_1\theta_2\theta_3 \rightarrow \pi-\theta_1, \pi+\theta_2, \theta_3$ (twofold axis parallel to **b**)

$\theta_1\theta_2\theta_3 \rightarrow \pi+\theta_1, \theta_2, \theta_3$ (twofold axis parallel to **c**).

(*b*) In the second crystal ($P2/m$):

$\theta_1\theta_2\theta_3 \rightarrow \pi+\theta_1, -\theta_2, \pi+\theta_3$ (onefold axis)

$\theta_1\theta_2\theta_3 \rightarrow \theta_1, \pi+\theta_2, \pi-\theta_3$ (twofold axis parallel to **b**).

When these symmetry operators are combined two cells result, each of which has the space group *Pbcb* (Fig. 2.3.6.5). The asymmetric unit within which the rotation function need be evaluated is found from a knowledge of the Eulerian space group. In the above example, the limits of the asymmetric unit are $0 \le \theta_1 \le \pi/2$, $0 \le \theta_2 \le \pi$ and $0 \le \theta_3 \le \pi/2$.

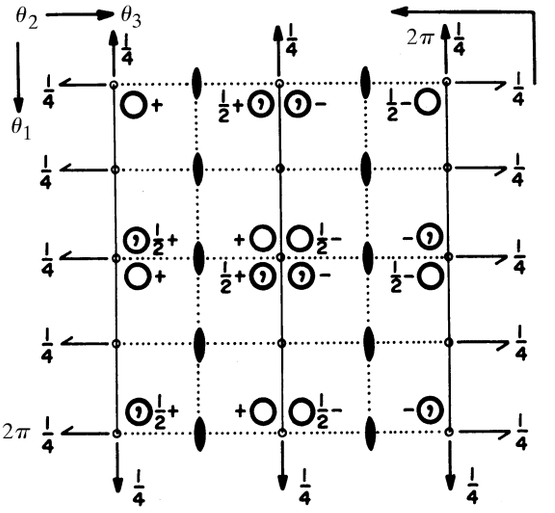

Fig. 2.3.6.5. Rotation space group diagram for the rotation function of a *Pmmm* Patterson function (P_1) against a $P2/m$ Patterson function (P_2). The Eulerian angles $\theta_1, \theta_2, \theta_3$ repeat themselves after an interval of 2π. Heights above the plane are given in fractions of a revolution. [Reprinted from Tollin *et al*. (1966).]

Non-linear transformations occur when using Eulerian symmetries for threefold axes along [111] (as in the cubic system) or when using polar coordinates. Hence, Eulerian angles are far more suitable for a derivation of the limits of the rotation-function asymmetric unit. However, when searching for given molecular axes, where some plane of κ need be explored, polar angles are more useful.

Rao *et al*. (1980) have determined all possible rotation function Eulerian space groups, except for combinations with Pattersons of cubic space groups. They numbered these rotation groups 1 through 100 (Table 2.3.6.3) according to the combination of the Patterson Laue groups. The characteristics of each of the 100 groups are given in Table 2.3.6.4, including the limits of the asymmetric unit. In the 100 unique combinations of non-cubic Laue groups, there are only 16 basic rotation function space groups.

2.3.6.4. *Sampling, background and interpretation*

If the origins are retained in the Pattersons, their product will form a high but constant plateau on which the rotation-function

Table 2.3.6.3. *Numbering of the rotation function space groups*

The Laue group of the rotated Patterson map P_1 is chosen from the left column and the Laue group of P_2 is chosen from the upper row.

	1	2/*m*, *b* axis unique	2/*m*, *c* axis unique	*mmm*	4/*m*	4/*mmm*	3	3*m*	6/*m*	6/*mmm*
1	1	11	21	31	41	51	61	71	81	91
2/*m*, *b* axis unique	2	12	22	32	42	52	62	72	82	92
2/*m*, *c* axis unique	3	13	23	33	43	53	63	73	83	93
mmm	4	14	24	34	44	54	64	74	84	94
4/*m*	5	15	25	35	45	55	65	75	85	95
4/*mmm*	6	16	26	36	46	56	66	76	86	96
3	7	17	27	37	47	57	67	77	87	97
3*m*	8	18	28	38	48	58	68	78	88	98
6/*m*	9	19	29	39	49	59	69	79	89	99
6/*mmm*	10	20	30	40	50	60	70	80	90	100

peaks are superimposed; this leads to a small apparent peak-to-noise ratio. The effect can be eliminated by removal of the origins through a modification of the Patterson coefficients. Irrespective of origin removal, a significant peak is one which is more than three r.m.s. deviations from the mean background.

As in all continuous functions sampled at discrete points, a convenient grid size must be chosen. Small intervals result in an excessive computing burden, while large intervals might miss peaks. Furthermore, equal increments of angles do not represent equal changes in rotation, which can result in distorted peaks (Lattman, 1972). In general, a crude idea of a useful sampling interval can be obtained by considering the angle necessary to move one reciprocal-lattice point onto its neighbour (separated by a^*) at the extremity of the resolution limit, R. This interval is given by

$$\Delta\theta = a^*/2(1/R) = \tfrac{1}{2}Ra^*.$$

Simple sharpening of the rotation function can be useful. This can be achieved by restricting the computations to a shell in reciprocal space or by using normalized structure factors. Useful limits are frequently 10 to 6 Å for an average protein or 6 to 5 Å for a virus structure determination.

When exploring the rotation function in polar coordinates, there is no significance to the latitude φ (Fig. 2.3.6.4) when $\psi = 0$. For small values of ψ, the rotation function will be quite insensitive to φ, which therefore needs to be explored only at coarse intervals (say 45°). As ψ approaches the equator at 90°, optimal increments of ψ and φ will be about equal. A similar situation exists with Eulerian angles. When $\theta_2 = 0$, the rotation function will be determined by $\theta_1 + \theta_3$, corresponding to $\psi = 0$ and varying κ in polar coordinates. There will be no dependence on $(\theta_1 - \theta_3)$. Thus Eulerian searches can often be performed more economically in terms of the variables $\eta = \theta_1 + \theta_3$ and $\Delta = \theta_1 - \theta_3$, where

$$[\boldsymbol{\rho}] = \begin{pmatrix} \left[\cos\eta\cos^2\left(\frac{\theta_2}{2}\right) + \cos\Delta\sin^2\left(\frac{\theta_2}{2}\right)\right] & \left[\sin\eta\cos^2\left(\frac{\theta_2}{2}\right) + \sin\Delta\sin^2\left(\frac{\theta_2}{2}\right)\right] & \sin\theta_2\sin(\eta-\Delta) \\ \left[-\sin\eta\cos^2\left(\frac{\theta_2}{2}\right) + \sin\Delta\sin^2\left(\frac{\theta_2}{2}\right)\right] & \left[\cos\eta\cos^2\left(\frac{\theta_2}{2}\right) - \cos\Delta\sin^2\left(\frac{\theta_2}{2}\right)\right] & \sin\theta_2\cos(\eta-\Delta) \\ \sin\theta_2\sin(\eta+\Delta) & -\sin\theta_2\cos(\eta+\Delta) & \cos\theta_2 \end{pmatrix},$$

which reduces to the simple rotation matrix

$$[\boldsymbol{\rho}] = \begin{pmatrix} \cos\eta & \sin\eta & 0 \\ -\sin\eta & \cos\eta & 0 \\ 0 & 0 & 1 \end{pmatrix}$$

when $\theta_2 = 0$.

The computational effort to explore carefully a complete asymmetric unit of the rotation-function Eulerian group can be considerable. However, unless improper rotations are under investigation (as, for example, cross-rotation functions between different crystal forms of the same molecule), it is not generally necessary to perform such a global search. The number of molecules per crystallographic asymmetric unit, or the number of subunits per molecule, are often good indicators as to the possible types of noncrystallographic symmetry element. For instance, in the early investigation of insulin, the rotation function was used to explore only the $\kappa = 180°$ plane in polar coordinates as there were only two molecules per crystallographic asymmetric unit (Dodson *et al.*, 1966). Rotation functions of viruses, containing 532 icosahedral symmetry, are usually limited to exploration of the $\kappa = 180, 120, 72$ and 144° planes [*e.g.* Rayment *et al.* (1978) and Arnold *et al.* (1984)].

In general, the interpretation of the rotation function is straightforward. However, noise often builds up relative to the signal in high-symmetry space groups or if the data are limited or poor. One aid to a systematic interpretation is the locked rotation function (Rossmann *et al.*, 1972) for use when a molecule has more than one noncrystallographic symmetry axis. It is then possible to determine the rotation-function values for each molecular axis for a chosen molecular orientation (Fig. 2.3.6.6).

Another problem in the interpretation of rotation functions is the appearance of apparent noncrystallographic symmetry that relates the self-Patterson of one molecule to the self-Patterson of a crystallographically related molecule. For example, take the case of α-chymotrypsin (Blow *et al.*, 1964). The space group is $P2_1$ with a molecular dimer in each of the two crystallographic asymmetric units. The noncrystallographic dimer axis was found to be perpendicular to the crystallographic 2_1 axis. The product of the crystallographic twofold in the Patterson with the orthogonal twofold in the self-Patterson vectors around the origin creates a third twofold, orthogonal to both of the other twofolds. In real space this represents a twofold screw direction relating the two dimers in the cell. In other cases, the product of the crystallographic and noncrystallographic symmetry results in symmetry which only has meaning in terms of all the vectors in the vicinity of the Patterson origin, but not in real space. Rotation-function peaks arising from such products are called Klug peaks (Johnson *et al.*, 1975). Such peaks normally refer to the total symmetry of all the vectors around the Patterson origin and may, therefore, be much larger than the peaks due to noncrystallographic symmetry within one molecule alone. Hence the Klug peaks, if not correctly recognized, can lead to erroneous conclusions (Åkervall *et al.*, 1972). Litvin (1975) has shown how Klug peaks can be predicted. These usually occur only for special orientations of a particle with a given symmetry relative to the crystallographic symmetry axes. Prediction of Klug peaks requires the simultaneous consideration of the noncrystallographic point group, the crystallographic point group and their relative orientations.

2.3.6.5. *The fast rotation function*

Unfortunately, the rotation-function computations can be extremely time-consuming by conventional methods. Sasada (1964) developed a technique for rapidly finding the maximum of

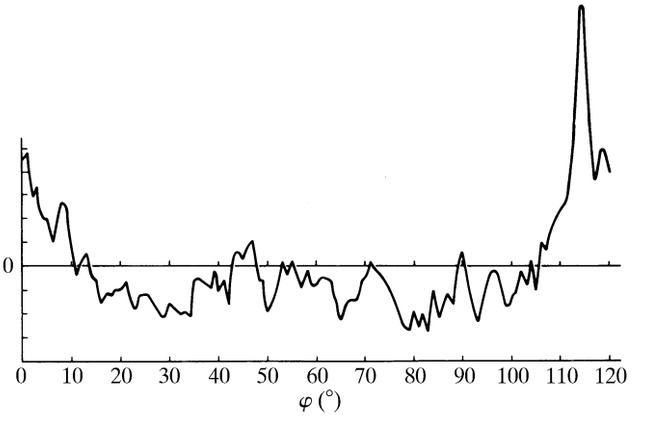

Fig. 2.3.6.6. The locked rotation function, L, applied to the determination of the orientation of the common cold virus (Arnold *et al.*, 1984). There are four virus particles per cubic cell with each particle sitting on a threefold axis. The locked rotation function explores all positions of rotation about this axis and, hence, repeats itself after 120°. The locked rotation function is determined from the individual rotation-function values of the noncrystallographic symmetry directions of a 532 icosahedron. [Reprinted with permission from Arnold *et al.* (1984).]

Table 2.3.6.4. *Rotation function Eulerian space groups*

The rotation space groups are given in Table 2.3.6.3.

No. of the rotation space group	No. of equivalent positions[a]	Symbol[b]	Translation along the θ_1 axis[c]	Translation along the θ_3 axis[c]	Range of the asymmetric unit[d]		
1	2	*Pn*	2π	2π	$0 \le \theta_1 < 2\pi$,	$0 \le \theta_2 \le \pi$,	$0 \le \theta_3 < 2\pi$
2	4	*Pbn*2_1	2π	2π	$0 \le \theta_1 < 2\pi$,	$0 \le \theta_2 \le \pi/2$,	$0 \le \theta_3 < 2\pi$
3	4	*Pc*	π	2π	$0 \le \theta_1 < \pi$,	$0 \le \theta_2 \le \pi$,	$0 \le \theta_3 < 2\pi$
4	8	*Pbc*2_1	π	2π	$0 \le \theta_1 < \pi$,	$0 \le \theta_2 \le \pi/2$,	$0 \le \theta_3 < 2\pi$
5	8	*Pc*	$\pi/2$	2π	$0 \le \theta_1 < \pi/2$,	$0 \le \theta_2 \le \pi$,	$0 \le \theta_3 < 2\pi$
6	16	*Pbc*2_1	$\pi/2$	2π	$0 \le \theta_1 < \pi/2$,	$0 \le \theta_2 \le \pi/2$,	$0 \le \theta_3 < 2\pi$
7	6	*Pn*	$2\pi/3$	2π	$0 \le \theta_1 < 2\pi/3$,	$0 \le \theta_2 \le \pi$,	$0 \le \theta_3 < 2\pi$
8	12	*Pbn*2_1	$2\pi/3$	2π	$0 \le \theta_1 < 2\pi/3$,	$0 \le \theta_2 \le \pi/2$,	$0 \le \theta_3 < 2\pi$
9	12	*Pc*	$\pi/3$	2π	$0 \le \theta_1 < \pi/3$,	$0 \le \theta_2 \le \pi$,	$0 \le \theta_3 < 2\pi$
10	24	*Pbc*2_1	$\pi/3$	2π	$0 \le \theta_1 < \pi/3$,	$0 \le \theta_2 \le \pi/2$,	$0 \le \theta_3 < 2\pi$
11	4	*P*2_1*nb*	2π	2π	$0 \le \theta_1 < 2\pi$,	$0 \le \theta_2 \le \pi/2$,	$0 \le \theta_3 < 2\pi$
12	8	*Pbnb*	2π	2π	$0 \le \theta_1 \le \pi/2$,	$0 \le \theta_2 < \pi$,	$0 \le \theta_3 < 2\pi$
13	8	*P*2*cb*	π	2π	$0 \le \theta_1 < \pi$,	$0 \le \theta_2 \le \pi/2$,	$0 \le \theta_3 < 2\pi$
14	16	*Pbcb*	π	2π	$0 \le \theta_1 \le \pi/2$,	$0 \le \theta_2 \le \pi/2$,	$0 \le \theta_3 < 2\pi$
15	16	*P*2*cb*	$\pi/2$	2π	$0 \le \theta_1 < \pi/2$,	$0 \le \theta_2 \le \pi/2$,	$0 \le \theta_3 < 2\pi$
16	32	*Pbcb*	$\pi/2$	2π	$0 \le \theta_1 < \pi/2$,	$0 \le \theta_2 < \pi$,	$0 \le \theta_3 \le \pi/2$
17	12	*P*2_1*nb*	$2\pi/3$	2π	$0 \le \theta_1 < 2\pi/3$,	$0 \le \theta_2 \le \pi/2$,	$0 \le \theta_3 < 2\pi$
18	24	*Pbnb*	$2\pi/3$	2π	$0 \le \theta_1 < 2\pi/3$,	$0 \le \theta_2 < \pi$,	$0 \le \theta_3 \le \pi/2$
19	24	*P*2*cb*	$\pi/3$	2π	$0 \le \theta_1 < \pi/3$,	$0 \le \theta_2 \le \pi/2$,	$0 \le \theta_3 < 2\pi$
20	48	*Pbcb*	$\pi/3$	2π	$0 \le \theta_1 < \pi/3$,	$0 \le \theta_2 < \pi$,	$0 \le \theta_3 \le \pi/2$
21	4	*Pa*	2π	π	$0 \le \theta_1 < 2\pi$,	$0 \le \theta_2 \le \pi$,	$0 \le \theta_3 < \pi$
22	8	*Pba*2	2π	π	$0 \le \theta_1 < 2\pi$,	$0 \le \theta_2 \le \pi/2$,	$0 \le \theta_3 < \pi$
23	8	*Pm*	π	π	$0 \le \theta_1 < \pi$,	$0 \le \theta_2 \le \pi$,	$0 \le \theta_3 < \pi$
24	16	*Pbm*2	π	π	$0 \le \theta_1 < \pi$,	$0 \le \theta_2 \le \pi/2$,	$0 \le \theta_3 < \pi$
25	16	*Pm*	$\pi/2$	π	$0 \le \theta_1 < \pi/2$,	$0 \le \theta_2 \le \pi$,	$0 \le \theta_3 < \pi$
26	32	*Pbm*2	$\pi/2$	π	$0 \le \theta_1 < \pi/2$,	$0 \le \theta_2 \le \pi/2$,	$0 \le \theta_3 < \pi$
27	12	*Pa*	$2\pi/3$	π	$0 \le \theta_1 < 2\pi/3$,	$0 \le \theta_2 \le \pi$,	$0 \le \theta_3 < \pi$
28	24	*Pba*2	$2\pi/3$	π	$0 \le \theta_1 < 2\pi/3$,	$0 \le \theta_2 \le \pi/2$,	$0 \le \theta_3 < \pi$
29	24	*Pm*	$\pi/3$	π	$0 \le \theta_1 < \pi/3$,	$0 \le \theta_2 \le \pi$,	$0 \le \theta_3 < \pi$
30	48	*Pbm*2	$\pi/3$	π	$0 \le \theta_1 < \pi/3$,	$0 \le \theta_2 \le \pi/2$,	$0 \le \theta_3 < \pi$
31	8	*P*2_1*ab*	2π	π	$0 \le \theta_1 < 2\pi$,	$0 \le \theta_2 \le \pi/2$,	$0 \le \theta_3 < \pi$
32	16	*Pbab*	2π	π	$0 \le \theta_1 \le \pi/2$,	$0 \le \theta_2 < \pi$,	$0 \le \theta_3 < \pi$
33	16	*P*2*mb*	π	π	$0 \le \theta_1 < \pi$,	$0 \le \theta_2 \le \pi/2$,	$0 \le \theta_3 < \pi$
34	32	*Pbmb*	π	π	$0 \le \theta_1 \le \pi/2$,	$0 \le \theta_2 \le \pi/2$,	$0 \le \theta_3 < \pi$
35	32	*P*2*mb*	$\pi/2$	π	$0 \le \theta_1 < \pi/2$,	$0 \le \theta_2 \le \pi/2$,	$0 \le \theta_3 < \pi$
36	64	*Pbmb*	$\pi/2$	π	$0 \le \theta_1 < \pi/2$,	$0 \le \theta_2 \le \pi/2$,	$0 \le \theta_3 \le \pi/2$
37	24	*P*2_1*ab*	$2\pi/3$	π	$0 \le \theta_1 < 2\pi/3$,	$0 \le \theta_2 \le \pi/2$,	$0 \le \theta_3 < \pi$
38	48	*Pbab*	$2\pi/3$	π	$0 \le \theta_1 < 2\pi/3$,	$0 \le \theta_2 \le \pi/2$,	$0 \le \theta_3 \le \pi/2$
39	48	*P*2*mb*	$\pi/3$	π	$0 \le \theta_1 < \pi/3$,	$0 \le \theta_2 \le \pi/2$,	$0 \le \theta_3 < \pi$
40	96	*Pbmb*	$\pi/3$	π	$0 \le \theta_1 < \pi/3$,	$0 \le \theta_2 \le \pi/2$,	$0 \le \theta_3 \le \pi/2$
41	8	*Pa*	2π	$\pi/2$	$0 \le \theta_1 < 2\pi$,	$0 \le \theta_2 \le \pi$,	$0 \le \theta_3 < \pi/2$
42	16	*Pba*2	2π	$\pi/2$	$0 \le \theta_1 < 2\pi$,	$0 \le \theta_2 \le \pi/2$,	$0 \le \theta_3 < \pi/2$
43	16	*Pm*	π	$\pi/2$	$0 \le \theta_1 < \pi$,	$0 \le \theta_2 \le \pi$,	$0 \le \theta_3 < \pi/2$
44	32	*Pbm*2	π	$\pi/2$	$0 \le \theta_1 < \pi$,	$0 \le \theta_2 \le \pi/2$,	$0 \le \theta_3 < \pi/2$
45	32	*Pm*	$\pi/2$	$\pi/2$	$0 \le \theta_1 < \pi/2$,	$0 \le \theta_2 \le \pi$,	$0 \le \theta_3 < \pi/2$
46	64	*Pbm*2	$\pi/2$	$\pi/2$	$0 \le \theta_1 < \pi/2$,	$0 \le \theta_2 \le \pi/2$,	$0 \le \theta_3 < \pi/2$
47	24	*Pa*	$2\pi/3$	$\pi/2$	$0 \le \theta_1 < 2\pi/3$,	$0 \le \theta_2 \le \pi$,	$0 \le \theta_3 < \pi/2$
48	48	*Pba*2	$2\pi/3$	$\pi/2$	$0 \le \theta_1 < 2\pi/3$,	$0 \le \theta_2 \le \pi/2$,	$0 \le \theta_3 < \pi/2$
49	48	*Pm*	$\pi/3$	$\pi/2$	$0 \le \theta_1 < \pi/3$,	$0 \le \theta_2 \le \pi$,	$0 \le \theta_3 < \pi/2$
50	96	*Pbm*2	$\pi/3$	$\pi/2$	$0 \le \theta_1 < \pi/3$,	$0 \le \theta_2 \le \pi/2$,	$0 \le \theta_3 < \pi/2$
51	16	*P*2_1*ab*	2π	$\pi/2$	$0 \le \theta_1 < 2\pi$,	$0 \le \theta_2 \le \pi/2$,	$0 \le \theta_3 < \pi/2$
52	32	*Pbab*	2π	$\pi/2$	$0 \le \theta_1 < 2\pi$,	$0 \le \theta_2 \le \pi/2$,	$0 \le \theta_3 \le \pi/4$
53	32	*P*2*mb*	π	$\pi/2$	$0 \le \theta_1 < \pi$,	$0 \le \theta_2 \le \pi/2$,	$0 \le \theta_3 < \pi/2$

Table 2.3.6.4. *Rotation function Eulerian space groups* (*cont.*)

No. of the rotation space group	No. of equivalent positions[(a)]	Symbol[(b)]	Translation along the θ_1 axis[(c)]	Translation along the θ_3 axis[(c)]	Range of the asymmetric unit[(d)]		
54	64	*Pbmb*	π	$\pi/2$	$0 \le \theta_1 \le \pi/2$,	$0 \le \theta_2 \le \pi/2$,	$0 \le \theta_3 < \pi/2$
55	64	*P*2*mb*	$\pi/2$	$\pi/2$	$0 \le \theta_1 < \pi/2$,	$0 \le \theta_2 \le \pi/2$,	$0 \le \theta_3 < \pi/2$
56	128	*Pbmb*	$\pi/2$	$\pi/2$	$0 \le \theta_1 \le \pi/4$,	$0 \le \theta_2 \le \pi/2$,	$0 \le \theta_3 < \pi/2$
57	48	$P2_1ab$	$2\pi/3$	$\pi/2$	$0 \le \theta_1 < 2\pi/3$,	$0 \le \theta_2 \le \pi/2$,	$0 \le \theta_3 < \pi/2$
58	96	*Pbab*	$2\pi/3$	$\pi/2$	$0 \le \theta_1 < 2\pi/3$,	$0 \le \theta_2 \le \pi/2$,	$0 \le \theta_3 \le \pi/4$
59	96	*P*2*mb*	$\pi/3$	$\pi/2$	$0 \le \theta_1 < \pi/3$,	$0 \le \theta_2 \le \pi/2$,	$0 \le \theta_3 < \pi/2$
60	192	*Pbmb*	$\pi/3$	$\pi/2$	$0 \le \theta_1 \le \pi/6$,	$0 \le \theta_2 \le \pi/2$,	$0 \le \theta_3 < \pi/2$
61	6	*Pn*	2π	$2\pi/3$	$0 \le \theta_1 < 2\pi$,	$0 \le \theta_2 \le \pi$,	$0 \le \theta_3 < 2\pi/3$
62	12	$Pbn2_1$	2π	$2\pi/3$	$0 \le \theta_1 < 2\pi$,	$0 \le \theta_2 \le \pi/2$,	$0 \le \theta_3 < 2\pi/3$
63	12	*Pc*	π	$2\pi/3$	$0 \le \theta_1 < \pi$,	$0 \le \theta_2 \le \pi$,	$0 \le \theta_3 < 2\pi/3$
64	24	$Pbc2_1$	π	$2\pi/3$	$0 \le \theta_1 < \pi$,	$0 \le \theta_2 \le \pi/2$,	$0 \le \theta_3 < 2\pi/3$
65	24	*Pc*	$\pi/2$	$2\pi/3$	$0 \le \theta_1 < \pi/2$,	$0 \le \theta_2 \le \pi$,	$0 \le \theta_3 < 2\pi/3$
66	48	$Pbc2_1$	$\pi/2$	$2\pi/3$	$0 \le \theta_1 < \pi/2$,	$0 \le \theta_2 \le \pi/2$,	$0 \le \theta_3 < 2\pi/3$
67	18	*Pn*	$2\pi/3$	$2\pi/3$	$0 \le \theta_1 < 2\pi/3$,	$0 \le \theta_2 \le \pi$,	$0 \le \theta_3 < 2\pi/3$
68	36	$Pbn2_1$	$2\pi/3$	$2\pi/3$	$0 \le \theta_1 < 2\pi/3$,	$0 \le \theta_2 \le \pi/2$,	$0 \le \theta_3 < 2\pi/3$
69	36	*Pc*	$\pi/3$	$2\pi/3$	$0 \le \theta_1 < \pi/3$,	$0 \le \theta_2 \le \pi$,	$0 \le \theta_3 < 2\pi/3$
70	72	$Pbc2_1$	$\pi/3$	$2\pi/3$	$0 \le \theta_1 < \pi/3$,	$0 \le \theta_2 \le \pi/2$,	$0 \le \theta_3 < 2\pi/3$
71	12	$P2_1nb$	2π	$2\pi/3$	$0 \le \theta_1 < 2\pi$,	$0 \le \theta_2 \le \pi/2$,	$0 \le \theta_3 < 2\pi/3$
72	24	*Pbnb*	2π	$2\pi/3$	$0 \le \theta_1 \le \pi/2$,	$0 \le \theta_2 < \pi$,	$0 \le \theta_3 < 2\pi/3$
73	24	*P*2*cb*	π	$2\pi/3$	$0 \le \theta_1 < \pi$,	$0 \le \theta_2 \le \pi/2$,	$0 \le \theta_3 < 2\pi/3$
74	48	*Pbcb*	π	$2\pi/3$	$0 \le \theta_1 \le \pi/2$,	$0 \le \theta_2 \le \pi/2$,	$0 \le \theta_3 < 2\pi/3$
75	48	*P*2*cb*	$\pi/2$	$2\pi/3$	$0 \le \theta_1 < \pi/2$,	$0 \le \theta_2 \le \pi/2$,	$0 \le \theta_3 < 2\pi/3$
76	96	*Pbcb*	$\pi/2$	$2\pi/3$	$0 \le \theta_1 \le \pi/4$,	$0 \le \theta_2 \le \pi/2$,	$0 \le \theta_3 < 2\pi/3$
77	36	$P2_1nb$	$2\pi/3$	$2\pi/3$	$0 \le \theta_1 < 2\pi/3$,	$0 \le \theta_2 \le \pi/2$,	$0 \le \theta_3 < 2\pi/3$
78	72	*Pbnb*	$2\pi/3$	$2\pi/3$	$0 \le \theta_1 \le \pi/6$,	$0 \le \theta_2 \le \pi$,	$0 \le \theta_3 < 2\pi/3$
79	72	*P*2*cb*	$\pi/3$	$2\pi/3$	$0 \le \theta_1 < \pi/3$,	$0 \le \theta_2 \le \pi/2$,	$0 \le \theta_3 < 2\pi/3$
80	144	*Pbcb*	$\pi/3$	$2\pi/3$	$0 \le \theta_1 \le \pi/6$,	$0 \le \theta_2 \le \pi/2$,	$0 \le \theta_3 < 2\pi/3$
81	12	*Pa*	2π	$\pi/3$	$0 \le \theta_1 < 2\pi$,	$0 \le \theta_2 \le \pi$,	$0 \le \theta_3 < \pi/3$
82	24	*Pba*2	2π	$\pi/3$	$0 \le \theta_1 < 2\pi$,	$0 \le \theta_2 \le \pi/2$,	$0 \le \theta_3 < \pi/3$
83	24	*Pm*	π	$\pi/3$	$0 \le \theta_1 < \pi$,	$0 \le \theta_2 \le \pi$,	$0 \le \theta_3 < \pi/3$
84	48	*Pbm*2	π	$\pi/3$	$0 \le \theta_1 < \pi$,	$0 \le \theta_2 \le \pi/2$,	$0 \le \theta_3 < \pi/3$
85	48	*Pm*	$\pi/2$	$\pi/3$	$0 \le \theta_1 < \pi/2$,	$0 \le \theta_2 \le \pi$,	$0 \le \theta_3 < \pi/3$
86	96	*Pbm*2	$\pi/2$	$\pi/3$	$0 \le \theta_1 < \pi/2$,	$0 \le \theta_2 \le \pi/2$,	$0 \le \theta_3 < \pi/3$
87	36	*Pa*	$2\pi/3$	$\pi/3$	$0 \le \theta_1 < 2\pi/3$,	$0 \le \theta_2 \le \pi$,	$0 \le \theta_3 < \pi/3$
88	72	*Pba*2	$2\pi/3$	$\pi/3$	$0 \le \theta_1 < 2\pi/3$,	$0 \le \theta_2 \le \pi/2$,	$0 \le \theta_3 < \pi/3$
89	72	*Pm*	$\pi/3$	$\pi/3$	$0 \le \theta_1 < \pi/3$,	$0 \le \theta_2 \le \pi$,	$0 \le \theta_3 < \pi/3$
90	144	*Pbm*2	$\pi/3$	$\pi/3$	$0 \le \theta_1 < \pi/3$,	$0 \le \theta_2 \le \pi/2$,	$0 \le \theta_3 < \pi/3$
91	24	$P2_1ab$	2π	$\pi/3$	$0 \le \theta_1 < 2\pi$,	$0 \le \theta_2 \le \pi/2$,	$0 \le \theta_3 < \pi/3$
92	48	*Pbab*	2π	$\pi/3$	$0 \le \theta_1 \le \pi/2$,	$0 \le \theta_2 < \pi$,	$0 \le \theta_3 < \pi/3$
93	48	*P*2*mb*	π	$\pi/3$	$0 \le \theta_1 < \pi$,	$0 \le \theta_2 \le \pi/2$,	$0 \le \theta_3 < \pi/3$
94	96	*Pbmb*	π	$\pi/3$	$0 \le \theta_1 \le \pi/2$,	$0 \le \theta_2 \le \pi/2$,	$0 \le \theta_3 \le \pi/2$
95	96	*P*2*mb*	$\pi/2$	$\pi/3$	$0 \le \theta_1 < \pi/2$,	$0 \le \theta_2 \le \pi/2$,	$0 \le \theta_3 < \pi/3$
96	192	*Pbmb*	$\pi/2$	$\pi/3$	$0 \le \theta_1 \le \pi/4$,	$0 \le \theta_2 \le \pi/2$,	$0 \le \theta_3 < \pi/3$
97	72	$P2_1ab$	$2\pi/3$	$\pi/3$	$0 \le \theta_1 < 2\pi/3$,	$0 \le \theta_2 \le \pi/2$,	$0 \le \theta_3 < \pi/3$
98	144	*Pbab*	$2\pi/3$	$\pi/3$	$0 \le \theta_1 < 2\pi/3$,	$0 \le \theta_2 \le \pi/2$,	$0 \le \theta_3 \le \pi/6$
99	144	*P*2*mb*	$\pi/3$	$\pi/3$	$0 \le \theta_1 < \pi/3$,	$0 \le \theta_2 \le \pi/2$,	$0 \le \theta_3 < \pi/3$
100	288	*Pbmb*	$\pi/3$	$\pi/3$	$0 \le \theta_1 \le \pi/6$,	$0 \le \theta_2 \le \pi/2$,	$0 \le \theta_3 < \pi/3$

Notes: (*a*) This is the number of equivalent positions in the rotation unit cell. (*b*) Each symbol retains the order $\theta_1, \theta_2, \theta_3$. The monoclinic space groups have the *b* axis unique setting. (*c*) This is a translation symmetry: *e.g.* for the case of $\pi/2$ translation along the θ_1 axis, $\theta_1, \theta_2, \theta_3$ goes to $\pi/2 + \theta_1, \theta_2, \theta_3$ and $\pi + \theta_1, \theta_2, \theta_3$, and $3\pi/2 + \theta_1, \theta_2, \theta_3$. All other equivalent positions in the basic rotation space group are similarly translated. (*d*) Several consistent sets of ranges exist but the one with the minimum range of θ_2 is listed.

a given peak by looking at the slope of the rotation function. A major breakthrough came when Crowther (1972) recast the rotation function in a manner suitable for rapid computation. Only a brief outline of Crowther's fast rotation function is given here. Details are found in the original text (Crowther, 1972) and his computer program description.

Since the rotation function correlates spherical volumes of a given Patterson density with rotated versions of either itself or another Patterson density, it is likely that a more natural form for the rotation function will involve spherical harmonics rather than the Fourier components $|\mathbf{F_h}|^2$ of the crystal representation. Thus, if the two Patterson densities $P_1(r,\psi,\varphi)$ and $P_2(r,\psi,\varphi)$ are expanded within the spherical volume of radius less than a limiting value of a, then

$$P_1(r,\psi,\varphi) = \sum_{lmn} a^*_{lmn}\, \hat{j}_l(k_{ln}r)\hat{Y}_l^{m^*}(\psi,\varphi)$$

and

$$P_2(r,\psi,\varphi) = \sum_{l'm'n'} b_{l'm'n'}\hat{j}_{l'}(k_{l'n'}r)\hat{Y}_{l'}^{m'}(\psi,\varphi),$$

and the rotation function would then be defined as

$$R = \int_{\text{sphere}} P_1(r,\psi,\varphi)\mathscr{R}P_2(r,\psi,\varphi)r^2\sin\psi\,\mathrm{d}r\,\mathrm{d}\psi\,\mathrm{d}\varphi.$$

Here $\hat{Y}_l^m(\psi,\varphi)$ is the normalized spherical harmonic of order l; $\hat{j}_l(k_{ln}r)$ is the normalized spherical Bessel function of order l; a_{lmn}, b_{lmn} are complex coefficients; and $\mathscr{R}P_2(r,\psi,\varphi)$ represents the rotated second Patterson. The rotated spherical harmonic can then be expressed in terms of the Eulerian angles $\theta_1,\theta_2,\theta_3$ as

$$\mathscr{R}(\theta_1,\theta_2,\theta_3)\hat{Y}_l^m(\psi,\varphi) = \sum_{q=-l}^{l} D^l_{qm}(\theta_1,\theta_2,\theta_3)\hat{Y}_l^q(\psi,\varphi),$$

where

$$D^l_{qm}(\theta_1,\theta_2,\theta_3) = \exp(iq\theta_3)d^l_{qm}(\theta_2)\exp(im\theta_1)$$

and $d^l_{qm}(\theta_2)$ are the matrix elements of the three-dimensional rotation group. It can then be shown that

$$R(\theta_1,\theta_2,\theta_3) = \sum_{lmm'n} a^*_{lmn}b_{lm'n}D^l_{m'm}(\theta_1,\theta_2,\theta_3).$$

Since the radial summation over n is independent of the rotation,

$$c_{lmm'} = \sum_n a^*_{lmn}b_{lmn},$$

and hence

$$R(\theta_1,\theta_2,\theta_3) = \sum_{lmm'} c_{lmm'}D^l_{m'm}(\theta_1,\theta_2,\theta_3)$$

or

$$R(\theta_1,\theta_2,\theta_3) = \sum_{mm'}\left[\sum_l c_{lmm'}d^l_{m'm}(\theta_2)\right]\exp[i(m'\theta_3 + m\theta_1)].$$

The coefficients $c_{lmm'}$ refer to a particular pair of Patterson densities and are independent of the rotation. The coefficients $D^l_{m'm}$, containing the whole rotational part, refer to rotations of spherical harmonics and are independent of the particular Patterson densities. Since the summations over m and m' represent a Fourier synthesis, rapid calculation is possible.

As polar coordinates rather than Eulerian angles provide a more graphic interpretation of the rotation function, Tanaka (1977) has recast the initial definition as

$$\begin{aligned} R(\theta_1,\theta_2,\theta_3) &= \int_{\text{sphere}} [\mathscr{R}(\theta_1,\theta_2,\theta_3=0)P_1(r,\psi,\varphi)] \\ &\quad\times[\mathscr{R}(\theta_1,\theta_2,\theta_3)P_2(r,\psi,\varphi)]\,\mathrm{d}V \\ &= \int_{\text{sphere}} [P_1(r,\psi,\varphi)][\mathscr{R}^{-1}(\theta_1,\theta_2,\theta_3=0) \\ &\quad\times\mathscr{R}(\theta_1,\theta_2,\theta_3)P_2(r,\psi,\varphi)]\,\mathrm{d}V. \end{aligned}$$

He showed that the polar coordinates are now equivalent to $\kappa=\theta_3$, $\psi=\theta_2$ and $\varphi=\theta_1-\pi/2$. The rotation function can then be expressed as

$$\begin{aligned} R(\kappa,\psi,\varphi) = \sum_{lmm'}\left(\sum_n a^*_{lmn}b_{lm'n}\right)\sum_q\{&d^l_{qm}(\psi)d^l_{qm'}(\psi)(-1)^{(m'-m)} \\ &\times\exp[i(\kappa q)]\exp[i(m'-m)\varphi]\}, \end{aligned}$$

permitting rapid calculation of the fast rotation function in polar coordinates.

Crowther (1972) uses the Eulerian angles α, β, γ which are related to those defined by Rossmann & Blow (1962) according to $\theta_1=\alpha+\pi/2$, $\theta_2=\beta$ and $\theta_3=\gamma-\pi/2$.

2.3.7. Translation functions

2.3.7.1. *Introduction*

The problem of determining the position of a noncrystallographic symmetry element in space, or the position of a molecule of known orientation in a unit cell, has been reviewed by Rossmann (1972), Colman *et al.* (1976), Karle (1976), Argos & Rossmann (1980), Harada *et al.* (1981) and Beurskens (1981). All methods depend on the prior knowledge of the object's orientation implied by the rotation matrix [$\boldsymbol{C}$]. The various translation functions, T, derived below, can only be computed given this information.

The general translation function can be defined as

$$T(\mathbf{S}_x,\mathbf{S}_{x'}) = \int_U \rho_1(\mathbf{x})\cdot\rho_2(\mathbf{x}')\,\mathrm{d}\mathbf{x},$$

where T is a six-variable function given by each of the three components that define $\mathbf{S}_x$ and $\mathbf{S}_{x'}$. Here $\mathbf{S}_x$ and $\mathbf{S}_{x'}$ are equivalent reference positions of the objects, whose densities are $\rho_1(\mathbf{x})$ and $\rho_2(\mathbf{x}')$. The translation function searches for the optimal overlap of the two objects after they have been similarly oriented. Following the same procedure used for the rotation-function derivation, Fourier summations are substituted for $\rho_1(\mathbf{x})$ and $\rho_2(\mathbf{x}')$. It can then be shown that

$$\begin{aligned} T(\mathbf{S}_x,\mathbf{S}_{x'}) = \int_U &\left\{\frac{1}{V_\mathbf{h}}\sum_\mathbf{h}|\mathbf{F_h}|\exp[i(\alpha_\mathbf{h}-2\pi\mathbf{h}\cdot\mathbf{x})]\right\} \\ &\times\left\{\frac{1}{V_\mathbf{p}}\sum_\mathbf{p}|\mathbf{F_p}|\exp[i(\alpha_\mathbf{p}-2\pi\mathbf{p}\cdot\mathbf{x}')]\right\}\mathrm{d}\mathbf{x}. \end{aligned}$$

Using the substitution $\mathbf{x}'=[\boldsymbol{C}]\mathbf{x}+\mathbf{d}$ and simplifying leads to

$$\begin{aligned} T(\mathbf{S}_x,\mathbf{S}'_x) = &\frac{1}{V_\mathbf{h}V_\mathbf{p}}\sum_\mathbf{h}\sum_\mathbf{p}|\mathbf{F_h}||\mathbf{F_p}| \\ &\times\exp[i(\alpha_\mathbf{h}+\alpha_\mathbf{p}-2\pi\mathbf{p}\cdot\mathbf{d})] \\ &\times\int_U\exp\{-2\pi i(\mathbf{h}+[\boldsymbol{C}]^T\mathbf{p})\cdot\mathbf{x}\}\,\mathrm{d}\mathbf{x}. \end{aligned}$$

The integral is the diffraction function $G_\mathbf{hp}$ (2.3.6.4). If the integration is taken over the volume U, centred at $\mathbf{S}_x$ and $\mathbf{S}_{x'}$, it follows that

references